Anti-Roll Tank Simulations with a Volume of Fluid (VOF) Based Navier-Stokes Solver

Daalen, E.F.G. van; Kleefsman, K.M.T.; Gerrits, J.; Luth, H.R.; Veldman, A.E.P.

Published in:
EPRINTS-BOOK-TITLE

Publication date:
2001

Twenty-Third Symposium on Naval Hydrodynamics (2001)

ANTI-ROLL TANK SIMULATIONS WITH A VOLUME OF FLUID (VOF) BASED NAVIER-STOKES SOLVER

E.F.G. van Daalen[1], K.M.T. Kleefsman[2], J. Gerrits[2], H.R. Luth[1], A.E.P. Veldman[2]
([1]MARIN, P.O. Box 28, 6700 AA Wageningen, The Netherlands,
[2]University of Groningen, Department of Mathematics,
P.O. Box 800, 9700 AV Groningen, The Netherlands)

ABSTRACT

Results of computer simulations of the water motion in ship anti-roll tanks are compared with experimental data. The numerical computations are done with a Volume Of Fluid (VOF) based Navier-Stokes solver. Both free-surface anti-roll tanks and U-tube anti-roll tanks are considered. Calculated and measured results for the local wave heights, the sway force and roll moment are presented for both regular and irregular tank motions. A simple but effective simulation model for the active control of U-tube anti-roll tanks is introduced. Finally, the fully nonlinear time-domain coupling of the ship motion and the tank water motion is established.

INTRODUCTION

A ship subjected to wind and wave forces will perform motions in six degrees of freedom, i.e. surge, sway, heave, roll, pitch and yaw. The roll motion is the most critical one because it is lightly damped and therefore prone to dynamic magnification, in particular in the resonance frequency range. Ship-roll stabilization has therefore received considerable attention; it still is a major subject of interest to ship designers and naval architects. Among a wide variety of roll-damping devices (Vasta *et al* 1961), anti-roll tanks are appreciated for their simplicity, low cost and action at low or even zero speed. The concept of using fluid tanks for ship-roll reduction was first conceived by Froude (1861). In the past, several types of anti-roll tanks have been proposed and tried in practice. Two basically different designs can be distinguished (see Fig. 1). Firstly, the free-surface anti-roll tank (Watts 1883, 1885), having one large free surface and secondly, the U-tube anti-roll tank (Frahm 1911), which has two smaller free surfaces. Theoretical studies on U-tube tanks are based on an equivalent double pendulum theory (Stigter 1966): the mass of the tank fluid can be regarded as a second pendulum attached to the pendulum representing the ship, over most of the roll frequency range. The physical behavior in a free-surface tank is completely different and must be classed in the group of shallow water waves (Verhagen & Van Wijngaarden 1965). Since the main stabilizing action is created by a bore travelling up and down the tank's width, the fluid flow is essentially nonlinear (Chu *et al* 1968). So, the basic principle the two anti-roll tank types have in common is the transfer of fluid from starboard to port side and vice versa, with a certain phase lag with respect to the ship's rolling motion; thus, a counteracting moment is provided. Sometimes a limited control is exerted over the motion of the fluid by installing restrictions or baffles in the center of the free-surface tank or in the duct and/or wing tanks of the U-tank. Active control is often applied to U-tanks by means of valves on top of the wing tanks or in a connecting air duct. Detailed descriptions of passive and active anti-roll tanks are due to Bell & Walker (1966) and Webster (1967). More recently, Lee & Vassalos (1996) investigated the stabilization effects of anti-roll tanks.

With the ongoing increase of computer resources and the improvement of numerical algorithms, experimental studies of fluid flow are more and more accompanied (or even replaced) by computer simulations. Nevertheless, experiments remain crucial for validation of Computational Fluid Dynamics (CFD) codes and a better physical understanding of fluid motion in complex geometries. Computer simulations of the fluid flow in anti-roll tanks are scarce. Zhong *et al* (1998) present results from two-dimensional simulations of a U-tube tank. The discretised Navier-Stokes equations are solved using the Galerkin scheme, based on the finite element method. The roll motion is assumed to be small, slow and sinusoidal. Furthermore, the flow is assumed to be laminar at all times. In the numerical model, the grid is kept fixed and the position of the free surface is specified as part of the boundary conditions; the grid does not move with the free surface. Simulations with various duct heights and wing-tank widths are discussed. Yamaguchi *et al*

(1995) simulate an impeller-activated U-tube tank. The Navier-Stokes equations are discretised using the SOLA-SURF scheme based on the finite difference method. The impeller is modeled as a velocity jump. The numerical simulations are done for a ship in regular waves. Unfortunately, these numerical models were not validated with experimental results.
The computer program ComFlo solves the Navier-Stokes equations for unsteady incompressible fluid flow in complex geometries. The method is based in part on the Volume Of Fluid (VOF) method (Hirt & Nichols 1981). ComFlo has found many applications in a wide variety of flow problems, ranging from fuel sloshing in space satellites (Gerrits *et al* 1999) to green water loading on the fore deck of a ship (Fekken *et al* 1999). The computational model has proven to be robust and accurate. Recently, an extensive validation program was set up and systematic series of computer simulations were performed for both free-surface type and U-tube type anti-roll tanks in regular and irregular motion. A selection from these results is presented here.

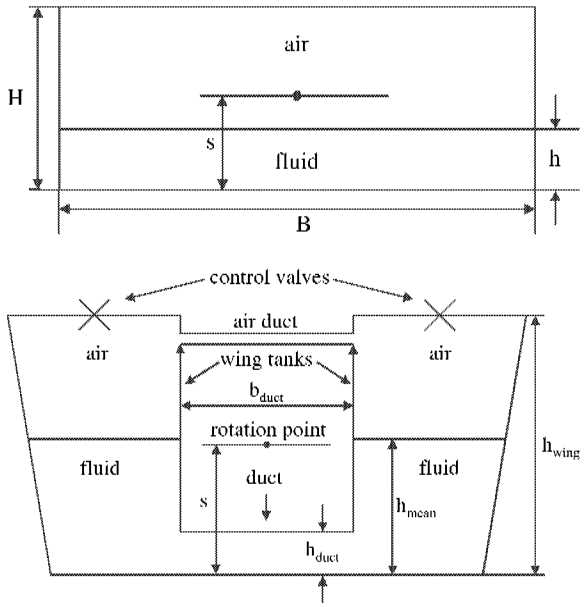

Figure 1: Definition of geometry and tank dimensions: free-surface anti-roll tank (top) and U-tube anti-roll tank (bottom).

The outline of this article is as follows: First of all, we briefly discuss the ComFlo program, in particular the underlying mathematical model and numerical method. Next, we focus on the tank fluid motion and the corresponding forces and moments. To this end, a series of computer simulations was carried out where the tank is given a prescribed rolling motion. The calculated results for the local wave heights and the forces and moments are compared with experimental data.
Next, the problem of active control for U-tanks is addressed. In practice, a simple and effective way to control the internal fluid motion is by closing and opening air valves located on top of the wing tanks. It is shown that by making use of the ideal gas law, the damping effect of the air volume above the fluid column can be taken into account. In this way, the fluid flow is blocked and the tank's roll peak period can be matched with the ship's natural period of roll.
Finally, the nonlinear coupling of the ship motion and the tank fluid motion is solved with a time domain method adopted from a numerical technique developed for nonlinear fluid sloshing in spinning containers (Gerrits & Veldman 2000).

COMFLO - MATHEMATICAL MODEL AND NUMERICAL METHOD

The motion of a fluid can be described by a set of partial differential equations expressing conservation of mass, momentum and energy per unit volume of the fluid. The Navier-Stokes equations for three-dimensional incompressible fluid flow can be written in conservation form as follows:

$$\nabla \cdot \vec{v} = 0 \tag{1}$$

$$\frac{\partial \vec{v}}{\partial t} + \nabla \cdot (\vec{v}\vec{v}^{T}) = -\frac{1}{\rho}\nabla p + \nu(\nabla \cdot \nabla)\vec{v} - g\vec{e}_3 \tag{2}$$

where

- $\vec{v}$ is the velocity field vector;
- p is the pressure;
- ρ is the mass density;
- ν is the kinematic viscosity;
- g is the acceleration of gravity;
- $\vec{e}_3$ is the unit vector pointing upwards;
- ∇ is the gradient operator;
- $\nabla \cdot$ is the divergence operator;
- $\nabla \cdot \nabla$ is the Laplace-operator;

On solid fixed boundaries either the no-slip condition

$$\vec{v} = \vec{0} \tag{3}$$

is used, or the free-slip conditions

$$v_n = \vec{v} \cdot \vec{n} = 0 \quad , \quad \tau = \frac{\partial v_t}{\partial n} = 0 \tag{4}$$

are imposed. In (4), v_n is the velocity component perpendicular to the solid fixed boundary, τ is the tangential stress and v_t is the tangential velocity component.
On the free surface the dynamic conditions hold, to ensure that (i) the free-surface pressure equals the atmospheric pressure and (ii) the air does not exert tangential forces on the free surface. These requirements are expressed as

$$\frac{p-p_0}{\rho} = \nu\frac{\partial v_n}{\partial n} - \frac{\sigma\kappa}{\rho} \quad , \quad \nu\left(\frac{\partial v_n}{\partial t} + \frac{\partial v_t}{\partial n}\right) = 0 \qquad (5)$$

where p_0 is the atmospheric pressure, σ is the surface tension and κ is the surface curvature. Usually, the first term on the right-hand side of (5) is neglected. A fixed Cartesian (rectilinear) grid is laid over the fluid domain. The discretization is based on a staggered grid: the pressure is calculated in the cell centers, whereas the velocity is calculated in the center of each cell face. Using so-called geometry and edge apertures (opening fractions), fluid domains of arbitrary shape can be handled. Each cell is assigned a cell label to distinguish between the fluid, the air, the fluid-air interface and the fluid domain boundaries. Finally, velocity labels are attributed to the cell faces to account for the various types of boundary conditions.
For integrating the time-dependent Navier-Stokes equations, the first order explicit forward Euler method was chosen. A predictor-corrector method was implemented in such a way that at all time levels the velocity field is divergence-free, in compliance with (1). The diffusive terms in (2) are discretized centrally and for the convective terms an upwind discretization is used. The Poisson equation for the pressure is solved by Successive Over-Relaxation. Finally, the free-surface profile is updated using a refined version of the so-called Donor-Acceptor algorithm (Sabeur *et al* 1998).
For a detailed description of ComFlo we refer to Gerrits (1996) and Loots (1997, 1998).

FREE-SURFACE TANKS IN REGULAR MOTION

Experiments were performed by Van den Bosch and Vugts (1966) to collect information about the performance of free-surface anti-roll tanks. A rectangular tank, partially filled with water, was forced to execute sinusoidal oscillations about a fixed axis while the moment due to the water motion was measured. From a harmonic analysis the moment amplitude A_M and phase angle ε_M with respect to the forced tank rolling motion $\phi(t)$ were determined. Systematic measurements were done for a wide range of tank parameters (tank width B, mean water depth h) and motion parameters (roll amplitude A_ϕ and frequency ω, height s of rotation point above tank floor). The tank length and height were kept constant at L=1m and H=0.5m respectively. The complete series of experiments was simulated with the program ComFlo (Van Daalen *et al* 1999).
When the water depth is large, the wave motion in the tank is a simple oscillation of the free surface for all frequencies. The fundamental mode of this standing wave has a length λ=2B. For shallow water, say for h/B < 0.1, the picture is entirely different. At low frequencies the (long) standing wave is present (Fig. 2a), but with increasing frequency very short progressive waves appear (Fig. 2b). In the transition regime the short waves interfere with the long wave. After these small disturbances the bore rises rather suddenly (Fig. 2c), while the phase lag between the water transfer and the imposed motion increases (see Fig. 3b); the quadrature component of the moment increases rapidly (Fig. 3c). Over a large frequency range the phenomenon does not change significantly, although the water motion becomes more violent and large vortices appear when the direction of wave propagation is reversed. Next, the bore passes into a solitary wave (Fig. 2d), a single steep wave running from one side of the tank to the other. After the bore has disappeared, the moment exerted by the water falls down rapidly (see Fig. 3a). With a small further increase in frequency the water approximates the "frozen" state (Fig. 2e) if the tank bottom is situated below the axis of rotation. When the tank is mounted above this axis, the water motion becomes rather chaotic. In this high frequency range there is hardly any water transfer.

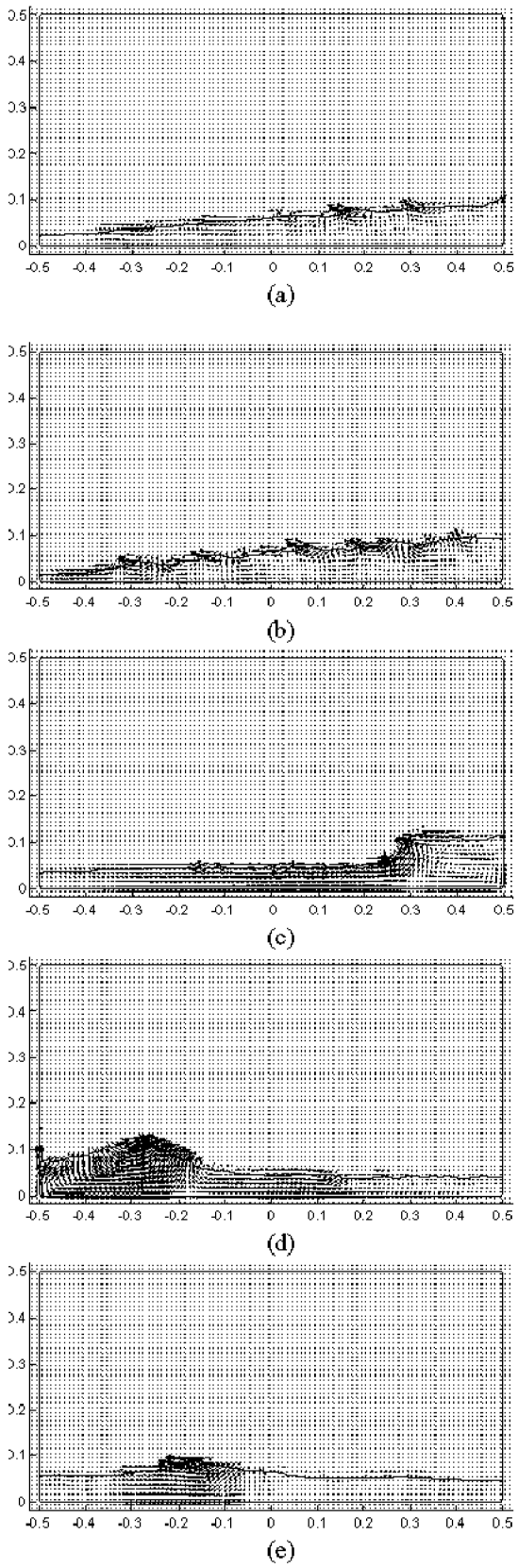

Figure 2 (left column): Free-surface tank in regular roll motion. Snapshots taken from computer simulations with ComFlo. Illustration of wave types for different frequency regimes: (a) standing wave; (b) standing wave and short travelling waves; (c) bore; (d) solitary wave; (e) frozen state.

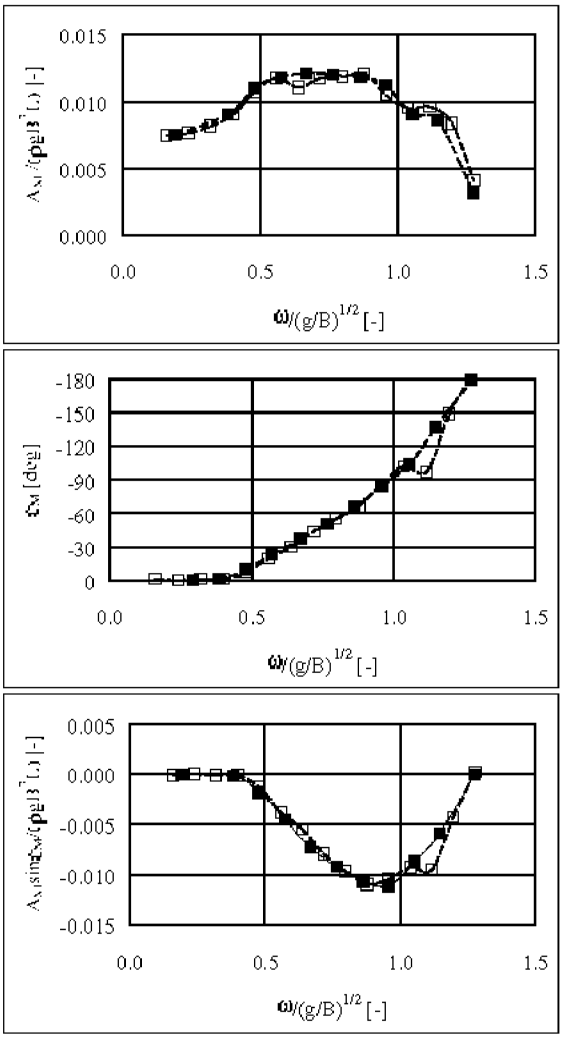

Figure 3: Free-surface tank in regular roll motion. Moment amplitude (top), phase angle (middle) and quadrature component (bottom) as function of roll frequency. Parameters: s/B=0.2, h/B=0.08, A_0=3.8deg. Closed squares: experiments; Open squares: ComFlo.

In the sequel we shall discuss the influence of each of the following tank and motion parameters separately: roll amplitude, mean water depth, height of rotation point above tank bottom and tank width. In the computer simulations, the grid has typically 40 cells in horizontal direction and 20 cells in vertical direction.

Figure 4 presents the non-dimensional moment amplitude $A_M/(\rho g B^3 L)$ and phase angle ε_M as function of the non-dimensional roll frequency $\omega/(g/B)^{1/2}$ for various values of the roll amplitude A_0. When the roll amplitude increases, the strength of the bore and thereby the moment amplitude increases too. This influences the phase angles as well. The increase in moment amplitude at the theoretical tank resonance frequency is not linear, but can be approximated by a square root expression (Verhagen & Van Wijngaarden 1965, Van Daalen & Westhuis 2000), as shown in Fig. 5.

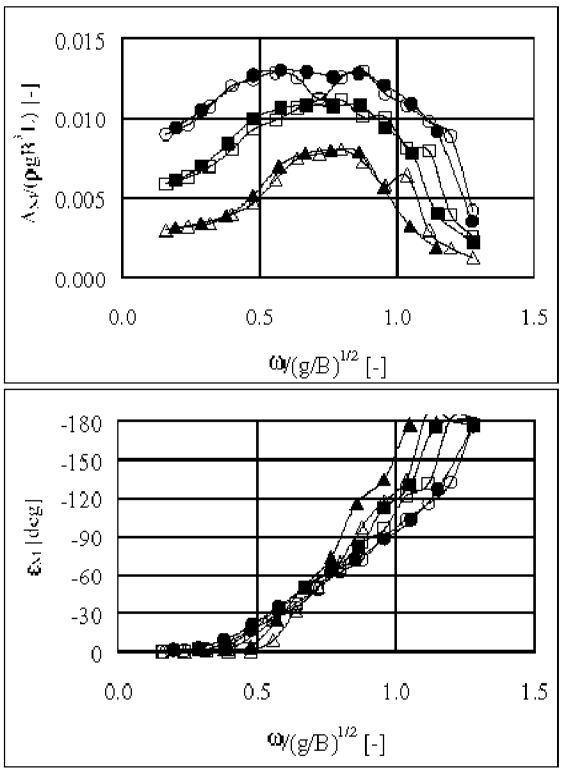

Figure 4: Free-surface tank in regular roll motion. Moment amplitude (top) and phase angle (bottom) as function of roll frequency. Parameters: s/B=0.0, h/B=0.06. Triangles: A_0=1.9deg; Squares: A_0=3.8deg; Circles: A_0=5.7deg. Closed symbols: experiments; Open symbols: ComFlo.

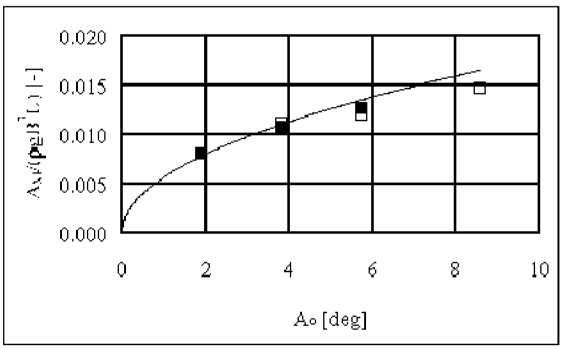

Figure 5: Free-surface tank in regular roll motion. Moment amplitude at theoretical resonance frequency as function of roll amplitude. Parameters: s/B=0.0; h/B=0.06. Line: theory; solid squares: experiments; open squares: ComFlo.

The mean water depth h is a particular important parameter, because it is clear that for a certain tank width B the only possibility to change the natural period of the water transfer, theoretically given by $T_0=2B/(gh)^{1/2}$, is by varying h. It is also clear that at or near this natural period the water transfer is largest and circumstances are most favorable for roll damping. The effect of increasing water depth is twofold: In the first place the curve of phase angles versus roll frequency is shifted to the higher frequency range, see Fig. 6 (middle). When the phase angles are plotted versus ω/ω_0, where $\omega_0=(\pi/B)(gh)^{1/2}$ is the tank's theoretical natural frequency, there is hardly any noticeable difference except for the higher frequencies (see Fig. 6 (bottom)), that is for the region in which the bore transforms into a solitary wave. In the second place the moment amplitude increases because of the larger amount of water in the tank, see Fig. 6 (top). Again, the increase at tank resonance is not linear, but can be approximated by a square root expression (Verhagen & Van Wijngaarden 1965, Van Daalen & Westhuis 2000), as shown in Fig. 7.

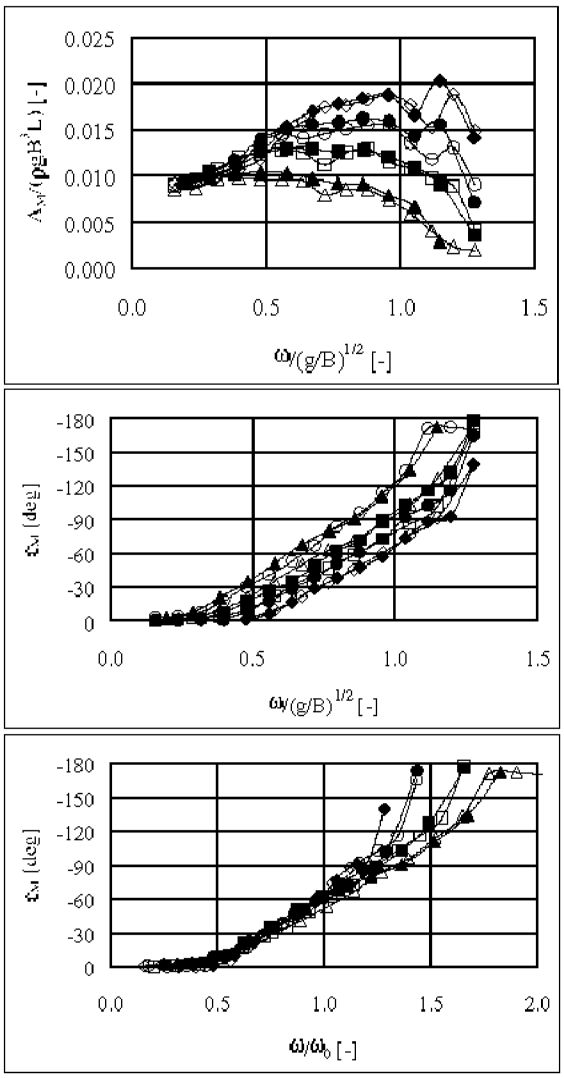

Figure 6: Free-surface tank in regular roll motion. Moment amplitude (top) and phase angle (middle and bottom) as function of roll frequency. Parameters: s/B=0.0; A_0=5.7deg. Triangles: h/B=0.04; Squares: h/B=0.06; Circles: h/B=0.08; Rhombs: h/B=0.10. Closed symbols: experiments; Open symbols: ComFlo.

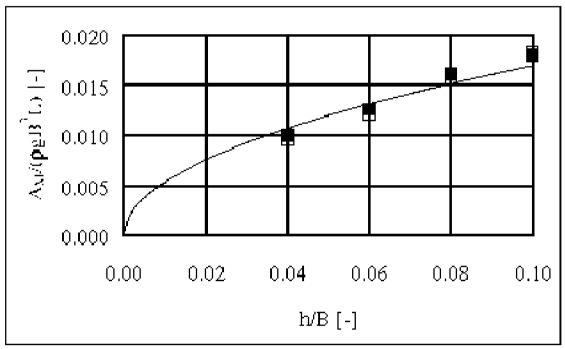

Figure 7: Free-surface tank in regular roll motion. Roll moment amplitude at theoretical resonance frequency as function of mean water depth. Parameters: s/B=0.0; A_0=5.7deg. Line: theory; Solid squares: experiments; Open squares: ComFlo.

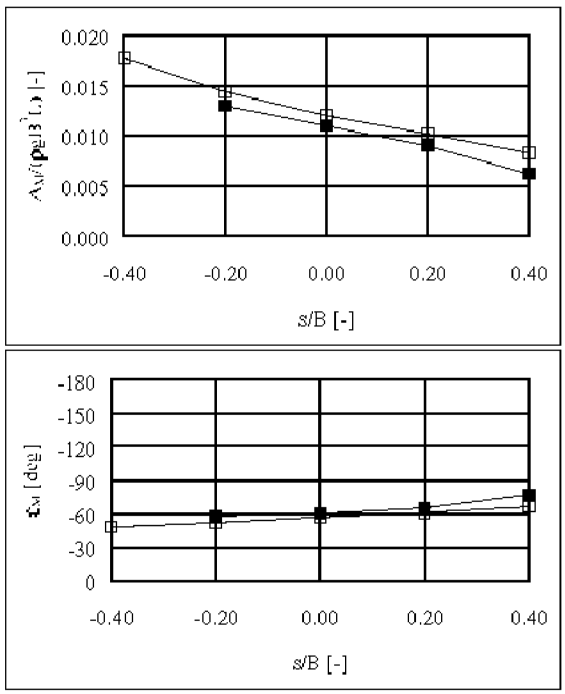

Figure 8: Free-surface tank in regular roll motion. Moment amplitude (top) and phase angle (bottom) at resonance frequency as function of rotation point height with respect to tank bottom. Parameters: h/B=0.06; A_0=5.7deg. Closed squares: experiments; Open squares: ComFlo.

The position of the tank with respect to the axis of rotation is another important design parameter. When the tank is mounted below the axis of rotation, the centrifugal force adds to the gravity force. When the tank is mounted above the rotation axis, the centrifugal force subtracts from the gravity force; the transverse acceleration is reversed as well. When the tank is situated at a higher level, the moment amplitude increases considerably (see Fig. 8 (top)), whereas the phase angle decreases but slightly (see Fig. 8 (bottom)). As a result, the quadrature component becomes larger and covers a wider frequency range, as shown in Fig. 9 (bottom).

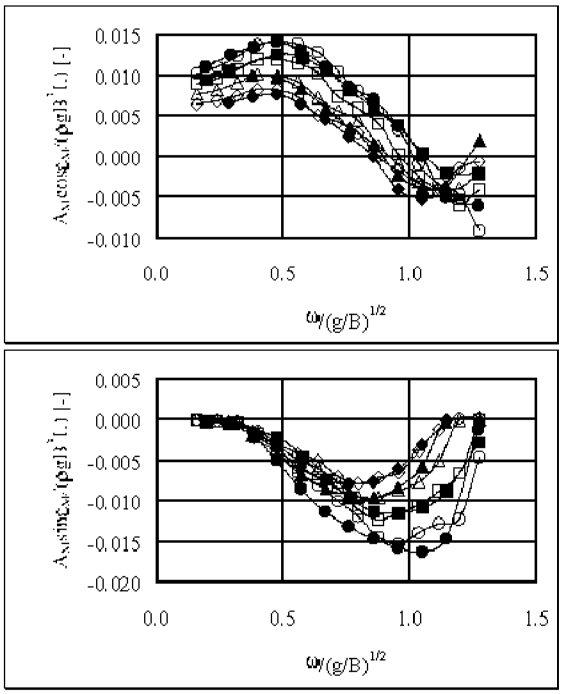

Figure 9: Free-surface tank in regular roll motion. In-phase (top) and quadrature (bottom) component of moment as function of roll frequency. Parameters: h/B=0.06; A_0=5.7deg. Rhombs: s/B=0.4; Squares: s/B=0.2; Triangles: s/B=0.0; Circles: s/B=-0.2. Closed symbols: experiments; Open symbols: ComFlo.

It can be expected that the moment exerted by the tank fluid is proportional to the fourth power of the model scale. Considering the moment per unit tank length in a two-dimensional problem, this will be proportional to the third power of the model scale, which in turn is governed by the tank width B. The fact that physically the phenomenon in the free-surface tank is a wave problem implies that for scaling up Froude's law of similitude applies; to create a comparable flow pattern the tanks should be filled according to the same value of h/B. When plotted in a non-dimensional way, it appears that the calculated results fully confirm these expectations, see Fig. 10.

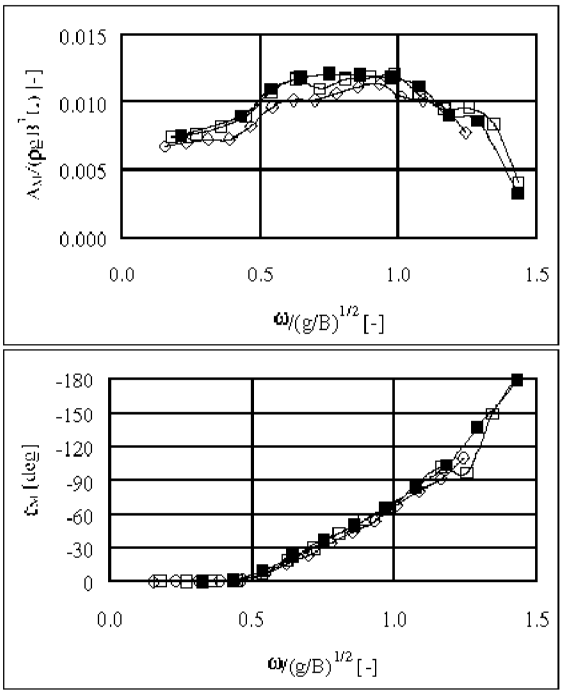

Figure 10: Free-surface tank in regular roll motion. Moment amplitude (top) and phase angle (bottom) as function of roll frequency. Parameters: s/B=0.2; h/B=0.08; A_0=5.7deg. Squares: B=1.00m; Rhombs: B=0.75m. Closed symbols: experiments; Open symbols: ComFlo.

U-TUBE TANKS IN REGULAR MOTION

A systematic series of tests with U-tube anti-roll tanks (see Fig. 11) in regular motion was conducted by Field & Martin (1976). The results of these experiments in terms of moment amplitude and phase angle were used to validate the ComFlo program. Three test cases with varying mean water depth were selected. The numerical simulations are done on a uniform grid with 100 cells in horizontal direction and 44 cells in vertical direction. The test parameters are given in Table 1:

Table 1: U-tank regular motion test parameters.

parameter	value	
L	5.334 m	17.5 ft
s	1.372 m	4.5 ft
b_{duct}	7.315 m	24 ft
h_{duct}	0.305 m	1 ft
b_{wing}	2.743 m	9 ft
h_{wing}	3.048 m	10 ft
h_{mean} – case 1	0.914 m	3 ft
h_{mean} – case 2	1.524 m	5 ft
h_{mean} – case 3	2.134 m	7 ft

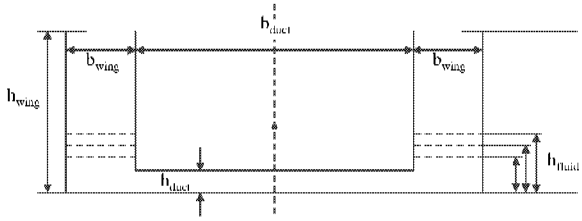

Figure 11: U-tube anti-roll tank (cross section).

Figures 12-14 show the moment amplitude and phase angle as function of the roll frequency. For all three test cases the calculated results are found to be in good agreement with the experimental data.

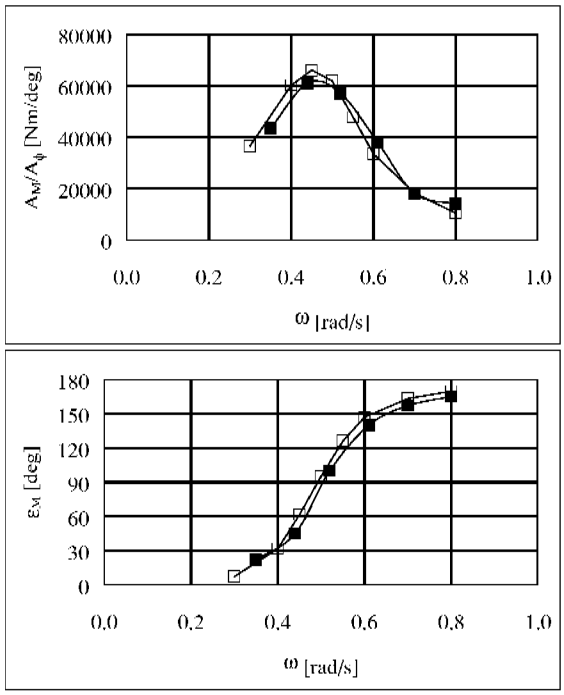

Figure 12: U-tank regular motion test. Case 1: h_{mean}=0.914m(=3ft). Moment amplitude (top) and phase angle (bottom) as function of roll frequency. Closed symbols: experiments; Open symbols: ComFlo.

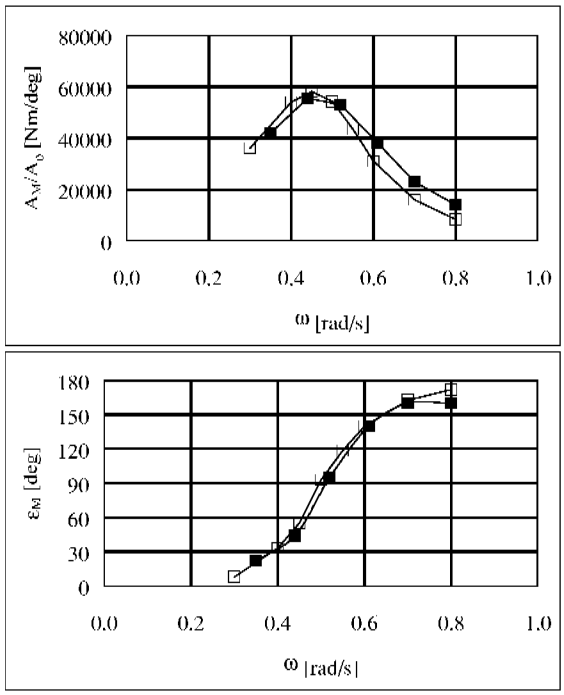

Figure 13: U-tank regular motion test. Case 2: h_{mean}=1.524m(=5ft). Moment amplitude (top) and phase angle (bottom) as function of roll frequency. Closed symbols: experiments; Open symbols: ComFlo.

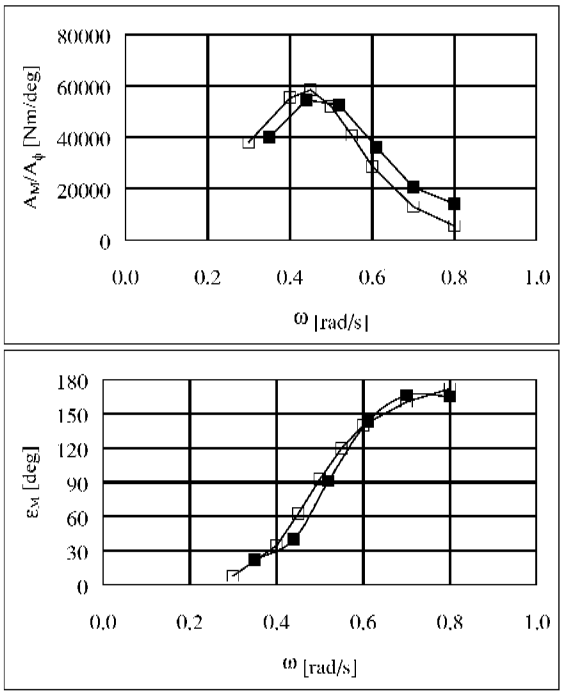

Figure 14: U-tank regular motion test. Case 3: h_{mean}=2.134m(=7ft). Moment amplitude (top) and phase angle (bottom) as function of roll frequency. Closed symbols: experiments; Open symbols: ComFlo.

U-TUBE TANKS IN IRREGULAR MOTION

Recently, tests were done in MARIN's former Seakeeping Basin with a ship model equipped with a U-tube anti-roll tank (Luth 1999). The water heights in both wing tanks and the sway force and roll moment exerted by the tank on the ship were measured during calm water roll decay tests and in irregular wave conditions. In the computer simulations, the measured sway, heave and roll motions were imposed on the tank (Kleefsman 2000). Figure 15 shows a cross-sectional view of the ship's hull and the U-tank.

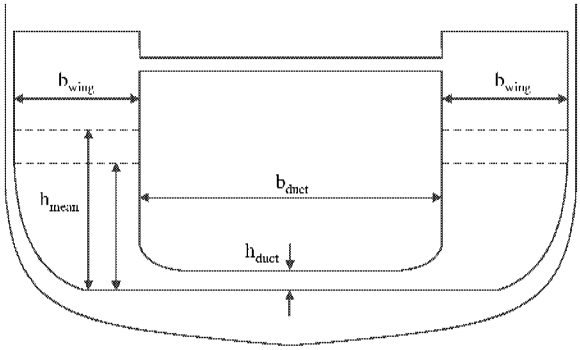

Figure 15: Ship with U-tank (cross section).

In the zero speed roll decay test, the ship is given an initial heel angle and is then released. The computer simulation is done with 200 cells in horizontal direction and 88 cells in vertical direction. The test parameters are given in Table 2:

Table 2: U-tank roll decay test parameters.

parameter	value
L	1.20 m
s	3.10 m
V_{fluid}	10.2 m^3
b_{wing}	1.95 m
b_{duct}	5.40 m
h_{duct}	0.25 m
h_{mean}	1.692 m
h_{PS}(t=0s) - h_{mean}	0.955 m
h_{SB}(t=0s) - h_{mean}	-0.993 m

Figure 16 shows the results in terms of the sway force and roll moment and the water height in the port-side wing tank. During the first three oscillations the agreement between calculated and measured results is good. When the amplitude of oscillation decreases, the agreement becomes less good. This is may be due to

- the absence of boundary layers; since the free-slip condition is applied at the wing tank and duct boundaries, boundary layers are not incorporated. Accurate modelling of the boundary layer flow would require a significant larger number of cells;
- the absence of a turbulence model in ComFlo.

The observed discrepancies call for further research.

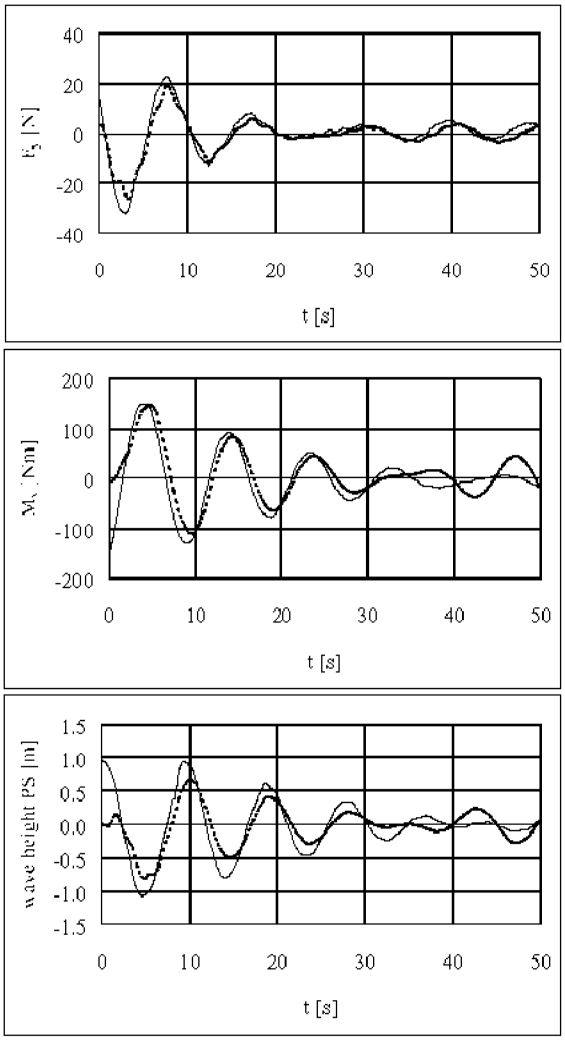

Figure 16: U-tank decay test. Sway force (top), roll moment (middle) and water height (bottom) in port-side wing tank as function of time. Solid line: experiments; Dashed line: ComFlo.

The computer simulation of the irregular wave test is done with 100 cells in horizontal direction and 44 cells in vertical direction. The test parameters which have changed with respect to the values in Table 2 are given in Table 3:

Table 3: U-tank irregular wave test parameters.

parameter	value
V_{fluid}	15.1 m^3
h_{mean}	2.652 m
$h_{PS}(t=0s) - h_{mean}$	-0.533 m
$h_{SB}(t=0s) - h_{mean}$	0.527 m

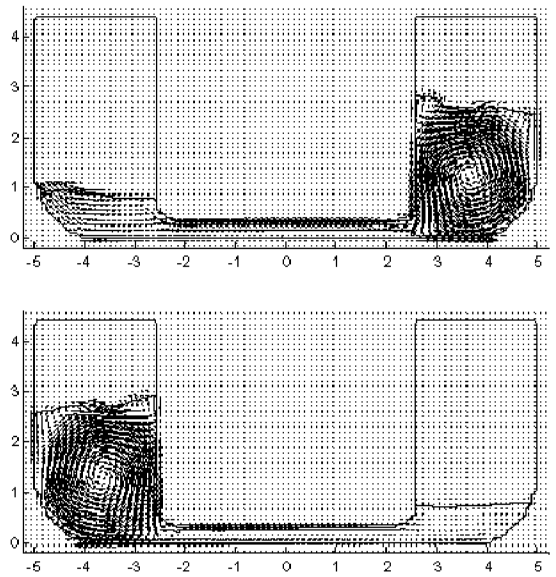

Figure 17: U-tank irregular wave test. Snapshots taken from simulations with ComFlo.

Figure 17 shows two snapshots taken from these simulations with the extreme water volumes in both wing tanks. Figure 18 shows the measured and calculated results. The agreement for the sway force is good, whereas the water height in the port-side wing tank and the roll moment (which are related quantities) are over-predicted.

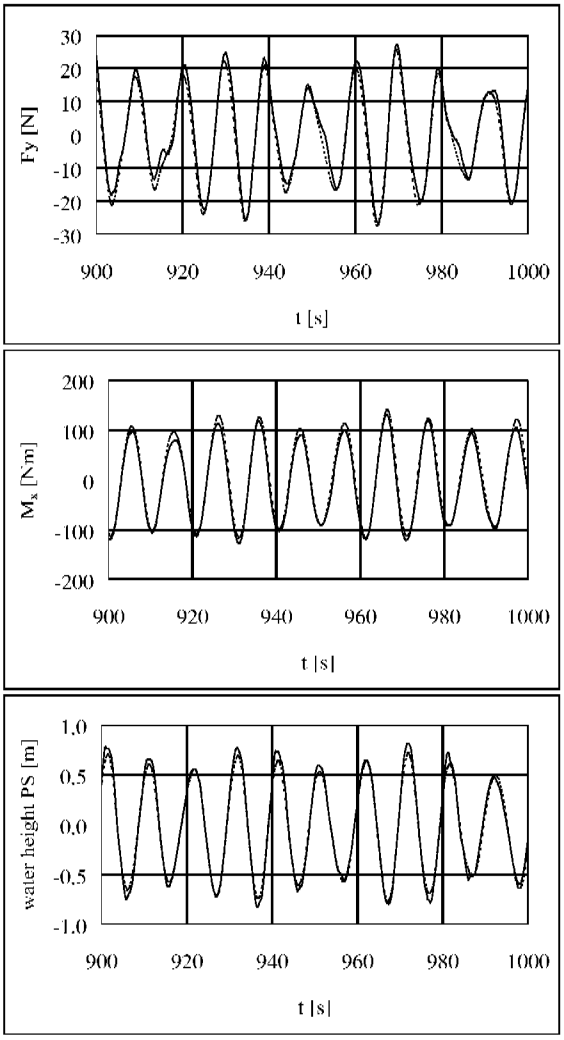

Figure 18: U-tank irregular wave test. Sway force (top), roll moment (middle) and water height in port-side wing tank (bottom) as function of time. Solid line: experiments; Dashed line: ComFlo.

U-TANKS WITH ACTIVE CONTROL

A major disadvantage of anti-roll tanks is that the free surface always reduces the metacentric height so that roll stability will be reduced. As a consequence, passive tanks amplify roll motions at low encounter frequencies. In certain circumstances this amplification may become a serious problem and it may be necessary to immobilise the tank by draining it or filling it completely. This will take a considerable time and passive tanks are therefore not suitable for ships, which are required to change, course frequently (e.g. warships). A solution may be found in the active control of the internal water motion. This is shown schematically in Fig. 19 for a U-tank.

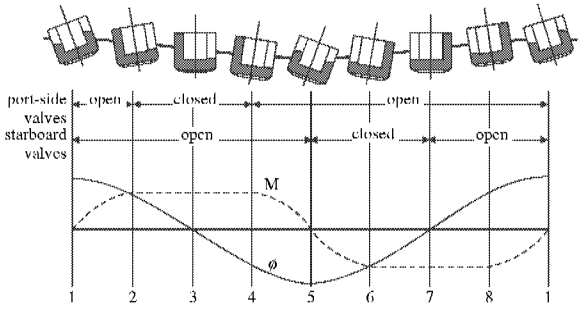

Figure 19: U-tank active control principle.

Stage 1 corresponds to the situation where the ship has reached the maximum angle to port and starts to right to starboard. At this stage the tank water is flowing with maximum velocity from starboard to port under the influence of gravity. When at stage 2 the tank water has obtained the maximum level in the port-side wing tank, the port-side valves are closed by the control. The ship continues to roll to starboard and – due to the closed port-side valves – the tank water is prevented from flowing into the low side tank, thus creating the stabilizing moment acting against the roll motion at stage 3. The water is kept blocked in the port-side wing tank, due to the low pressure created in the upper part of the wing tank, from stage 2 until stage 4. At stage 4 the control opens the port-side valves. This enables the water to flow from port side into the starboard wing tank. At stage 5 when the ship has obtained its maximum roll angle to starboard, the tank water is flowing with maximum velocity into the starboard wing tank. After stage 5 the ship starts to right to port while the tank water continues to flow to starboard to reach its maximum level at stage 6. At stage 6 the starboard valves are closed in order to prevent the tank water from flowing back to port side. Between stages 6 and 8, the blocked water on the upwards moving ship's side produces the stabilizing effect. At stage 8 the control opens the starboard valves, the tank water flows from starboard to port side and the cycle starts once more.

In ComFlo, the active control is modeled on the basis of the ideal gas law, which states that for a gas in a closed container at constant temperature, the product of pressure and the volume is constant. Suppose that at stage 2, when the water has reached its maximum level in the port-side wing tank, the pressure is given by p_0 and the volume of air above the water by V_0. Somewhat further in time, the air volume will have changed (due to the water motion) to $V=V_0+\Delta V$ and the corresponding change in pressure Δp can be obtained from

$$(p_0 + \Delta p)(V_0 + \Delta V) = p_0 V_0 \qquad (6)$$

or, in first order approximation,

$$\Delta p = -p_0 \frac{\Delta V}{V_0} \qquad (7)$$

The change in air pressure is then used in the dynamic free-surface condition to account for the effect of the closed valves. In this way, the water is blocked for a certain delay time ΔT.

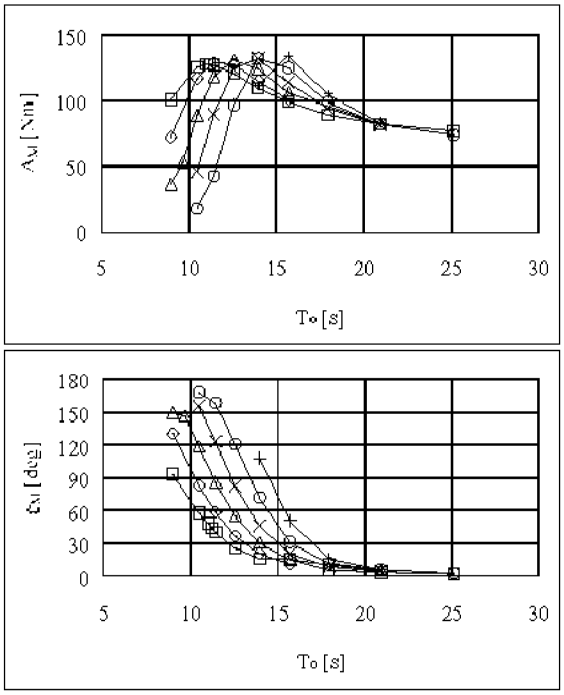

Figure 20: U-tank manual control test. Moment amplitude (top) and phase angle (bottom) as function of roll period. Parameters: A_0=4.9deg. Squares: ΔT=0.0s; Rhombs: ΔT=0.5s; Triangles: ΔT=1.0s; Crosses: ΔT=1.5s; Circles: ΔT=2.0s; Plusses: ΔT=2.5s.

Figure 20 shows the calculated moment amplitude as function of roll frequency for various values of the delay time ΔT. The natural frequency of the tank is ω_0=0.56rad/s, which corresponds to a natural period T_0=11.2s. A sinusoidal rolling motion is imposed on the U-tank. When the water reaches it maximum height in either one of the wing tanks, it was blocked by means of the above procedure. The delay time ΔT was varied (manually) from 0 to 2.5 seconds with increment 0.5s. In this way, the tank's peak period (i.e. the period at which the moment amplitude has its maximum) can be increased. For instance, if the ship's roll frequency equals ω=0.40rad/s, the delay time must be set to ΔT=2.5s, according to Fig. 20. Indeed, the exact delay time is given by $\Delta T^*=(2\pi/\omega - T_0)/2$ which yields ΔT^*=2.3s.

Figure 21 shows the velocity field and the free-surface profile in a U-tank with active control. The snapshots are taken at the time stages where the valves are closed and opened.

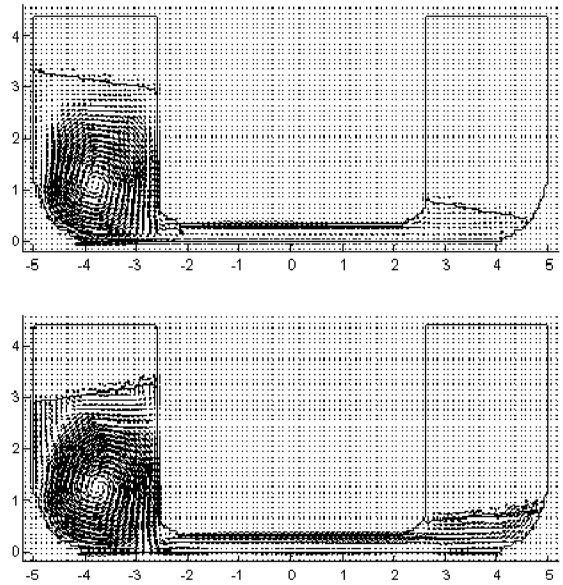

Figure 21: U-tank active control simulation. Snapshots taken from simulation with ComFlo. Velocity field and free-surface profile at time of closing (top) and opening (bottom) of the valves.

From the above it is clear that the delay time ΔT can be used to match the peak period of the water motion to the ship's roll period. To this end, ΔT is set to

$$\Delta T = t_{open} - t_{close} = 2(t_{V=V_{max}} - t_{\phi=0}) \qquad (8)$$

where $t_{V=V_{max}}$ denotes the time stage at which the wing tank volumes are extremal and $t_{\phi=0}$ denotes the time stage at which the ship is in it's upright position. Figure 22 shows the roll moment as function of time for the U-tank in semi-irregular motion (a superposition of harmonic components). Clearly, the moment amplitude is effectively increased by the control, as a direct consequence of the increased maximum water-height amplitudes in the wing tanks. The delay intervals are recognized as horizontal sections in the graphs of the water volume in the port-side wing tank and the duct flow rate.

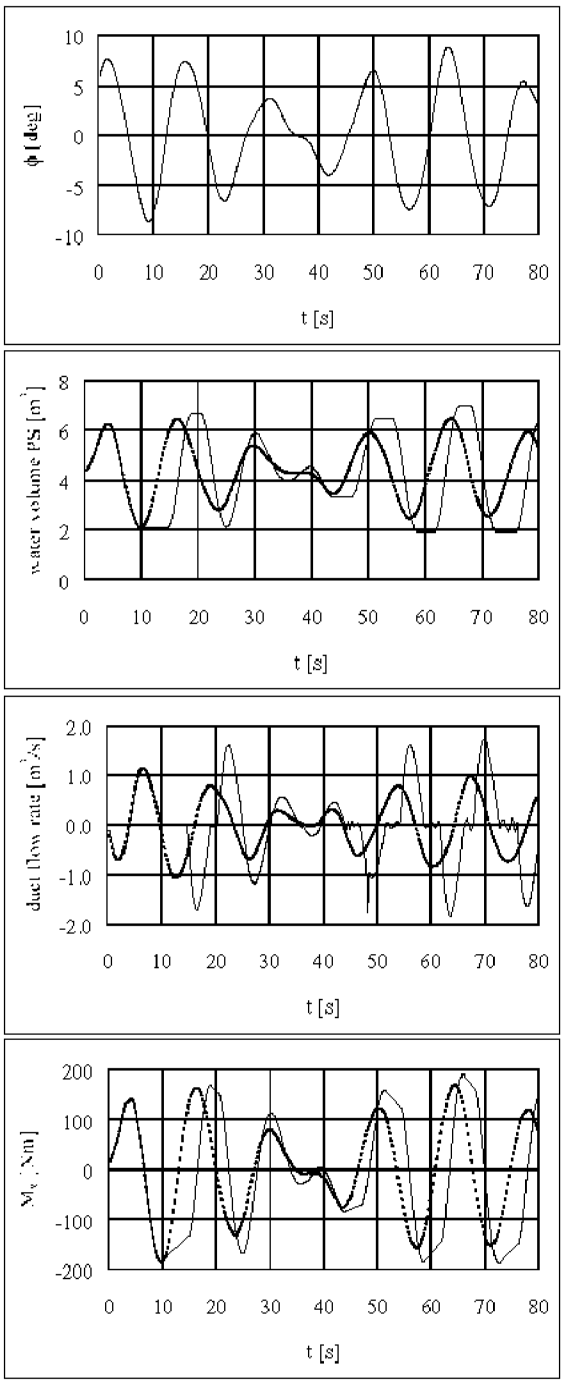

Figure 22: U-tank active control test. From top to bottom: roll angle, water volume in port-side wing tank, duct flow rate and moment versus time. Dashed line: no control; Solid line: active control.

COUPLED SHIP AND TANK FLUID MOTION

In a coupled system of a ship equipped with an anti-roll tank, the ship reacts to the forces of the waves and the action of the tank fluid. The tank fluid, in its turn, will be influenced directly by the motion of the ship. This interaction is essentially nonlinear and must therefore be solved in the time domain. A similar approach was followed by Armenio et al (1996) for a ship with partially filled baffled and unbaffled tanks.

The motion of the water in the U-tank is governed by equations (1) and (2). The frequency domain equations of motion for the coupled ship-tank system express the conservation of linear and angular momentum, i.e.

$$(M+A)\ddot{\vec{x}}+B\dot{\vec{x}}+C\vec{x}=\vec{F}^{exc}+\vec{F}^{rad}+\vec{F}^{tank} \qquad (9)$$

where $\vec{x}$ is the 6-component vector with the ship's translations (surge, sway and heave) and rotations (roll, pitch and yaw), M is the (6×6)-mass matrix, A, B and C are (6×6)-matrices with the frequency-dependent added mass, damping and spring coefficients, $\vec{F}^{exc}$ is a 6-component vector with the forces and moments due to the incoming and diffracted waves and $\vec{F}^{rad}$ is the contribution from the radiated waves. The incoming and diffracted wave contributions are calculated with MARIN's strip theory program SHIPMO (1998). The radiated wave contributions are expressed as convolution integrals involving the so-called retardation functions and the time history of the ship's velocities:

$$\vec{F}^{rad}(t)=-A^{\infty}\ddot{\vec{x}}(t)-B^{\infty}\dot{\vec{x}}(t)-\int_0^t K(t-\tau)\dot{\vec{x}}(\tau)d\tau \qquad (10)$$

The time-dependent retardation functions K(t) are computed from the frequency-dependent damping coefficients $B(\omega)$:

$$K(t)=\int_0^{\infty}\left[B(\omega)-B^{\infty}\right]\cos\omega t\,d\omega \qquad (11)$$

where B^{∞} is the (6×6)-matrix with the limiting values of the damping coefficients for infinite frequency.

The equations of motion (time domain) are then re-arranged as follows:

$$(M+A^{\infty})\ddot{x}(t) = -B^{\infty}\dot{x}(t) - \int_0^t K(t-\tau)\dot{x}(\tau)d\tau - Cx(t) + F^{exc}(t) + F^{tank}(t) \quad (12)$$

The forces and moments due to the internal water motion in the tank are obtained by integrating the pressure and shear stresses over the tank boundary S:

$$F_i^{tank} = \iint_S ((pI - \mu\nabla v)n)_i \, dS \quad , \quad i = 1,2,3 \quad (13)$$

$$F_i^{tank} = \iint_S ((r \times (pI - \mu\nabla v)) \cdot n)_i \, dS \quad , \quad i = 4,5,6 \quad (14)$$

where I is the (3×3)-identity matrix, μ is the dynamic fluid viscosity, n is the outward pointing normal vector on S and $r = x - x_G$ is the position vector with respect to the ship's center of gravity G.

The equations of motion of the ship are re-arranged such that the "dead weight" of the tank water is shifted to the left-hand side of (12), whereas the momentum contributions due to the internal dynamics remain on the right-hand side. In this way, a numerically stable time integration scheme is obtained when, for example, a fourth order Runge-Kutta method is applied (Gerrits & Veldman 2000).

Figure 23 shows the computed rolling motion of a ship with an empty U-tank and a partially filled U-tank. The ship is excited in rolling motion by the incoming waves at a frequency ω = 0.60rad/s. The natural frequency of the U-tank is ω_0 = 0.56rad/s. Clearly, the U-tank dampens the ship's roll amplitude by some 50%. Figure 24 shows the moment contributions due to the wave excitation and the U-tank.

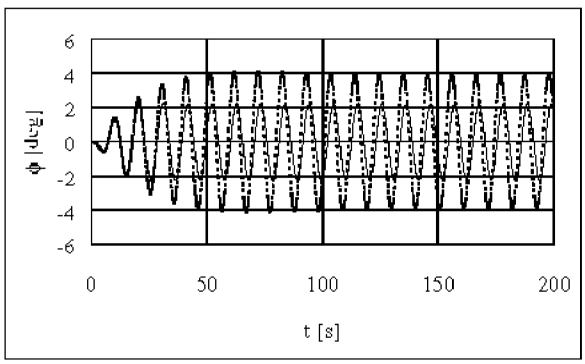

Figure 23: Coupled ship-U-tank simulation. Roll angle versus time. Solid line: partially filled tank; Dashed line: empty tank.

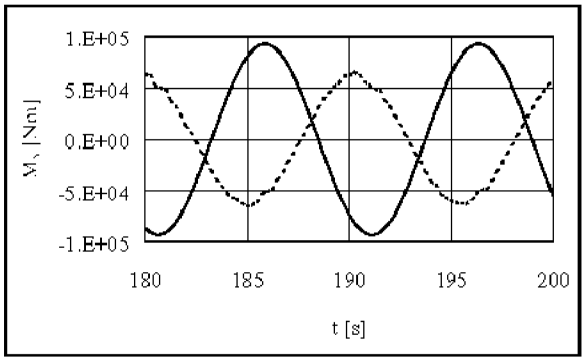

Figure 24: Coupled ship-U-tank simulation. Roll moment contributions: solid line = wave excitation; dashed line = U-tank.

COUPLED SHIP AND TANK FLUID MOTION WITH ACTIVE CONTROL

Finally, we present the results from a computer simulation where the coupling model and the control model are combined. Figure 25 shows the results from a simulation for ω=0.45rad/s, i.e. off tank resonance. Three configurations were simulated: (1) ship with empty tank; (2) ship with partially filled tank without control; (3) ship with partially filled tank and active control. It can be observed that the passive (uncontrolled) U-tank (configuration 2) increases the roll amplitude by some 15% with respect to configuration 1, whereas the active (controlled) U-tank (configuration 3) reduces the roll amplitude by some 10%.

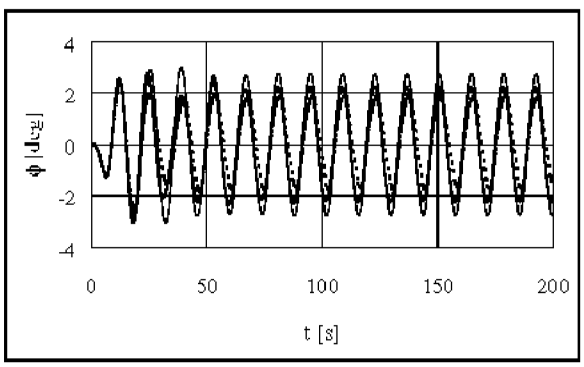

Figure 25: Coupled ship-U-tank simulation. Roll angle versus time. Solid thick line: empty tank; Solid thin line: partially filled tank, no control; Dashed thick line: partially filled tank, active control.

CONCLUSIONS

We have presented results from the application of the computer program ComFlo to the problem of water sloshing in free-surface and U-tube anti-roll tanks. The measured and calculated results for the water heights, the sway force and roll-moment amplitudes and phases were found to be in good agreement.
A simple simulation model for active control was introduced and found to be an effective means for tuning the tank's peak period to the ship's roll behavior. Better control models will be implemented.
Results obtained with a stable time integration scheme for the coupled equations of motion for the ship and the tank fluid were presented. In combination with the active control model, this scheme facilitates the simulation of 6DOF ship motions in a seaway with fully nonlinear account of the anti-roll tank fluid dynamics.
In the near future the effect of coupled sway-roll motions will be investigated, both numerically and experimentally. Another step in the validation process is the simulation of three-dimensional fluid motion in anti-roll tanks, taking into account internal geometries (Van Daalen *et al* 2000).

REFERENCES

Armenio, V., Francescutto, A., La Rocca, M., "On the roll motion of a ship with partially filled unbaffled and baffled tanks – Part I: Mathematical model and experimental setup", International Journal of Offshore and Polar Engineering, Vol. 6, No. 4, 1996, pp. 278-282.

Armenio, V., Francescutto, A., La Rocca, M., "On the roll motion of a ship with partially filled unbaffled and baffled tanks – Part II: Numerical and experimental analysis", International Journal of Offshore and Polar Engineering, Vol. 6, No. 4, 1996, pp. 283-290.

Bell, J. and Walker, W.P., "Activated and passive controlled fluid tank system for ship stabilization", Transactions of the Society of Naval Architects and Marine Engineers (SNAME), Vol. 75, 1966, pp. 1-22.

Bosch, J.J. van den and Vugts, J.H., "Roll damping by free surface tanks", Shipbuilding Laboratory of the Technical University of Delft, Report No. 83S, 1966.

Chu, W.H., Dalzell, J.F. and Modisette, J.E., "Theoretical and experimental study of ship-roll stabilization tanks", Journal of Ship Research, Vol. 12, 1968, pp. 165-180.

Daalen, E.F.G. van, Doeveren, A.G. van, Driessen, P.C.M., and Visser, C., "Two-dimensional free surface anti-roll tank simulations with a Volume Of Fluid based Navier-Stokes solver", Maritime Research Institute Netherlands, Report No. 15306-1-OE, October 1999.

Daalen, E.F.G. van, Gerrits, J., Loots, G.E. and Veldman, A.E.P., "Free surface anti-roll tank simulations with a Volume Of Fluid based Navier-Stokes solver", Proceedings of the 15th International Workshop on Water Waves and Floating Bodies, Caesarea, Israel, 2000, pp. 32-35.

Daalen, E.F.G. van and Palazzi, L., "3D fluid sloshing in rectangular containers – Validation of a Volume Of Fluid based Navier-Stokes solver", Maritime Research Institute Netherlands, Report No. 16131-2-RD, May 2000.

Daalen, E.F.G. van and Westhuis, J.-H., "Non-linear oscillations of fluid in a rectangular container – Validation of a first order perturbation analysis based on the non-linear shallow water theory", Maritime Research Institute Netherlands, Report No. 16131-1-RD, March 2000.

Fekken, G., Veldman, A.E.P., and Buchner, B., "Simulation of green-water loading using the Navier-Stokes equations", Proceedings of the 7th International Conference on Numerical Ship Hydrodynamics, Nantes (France), 1999.

Field, S.B. and Martin, J.P., "Comparative effects of U-tube and free surface type passive roll stabilization systems", Transactions of the Royal Institution of Naval Architects, Vol. 118, 1976, pp. 73-92.

Frahm, H., "Neuartige Schlingertanks zur Abdämpfung von Schiffrollbewegungen und ihre erfolgreiche Anwendung in der Praxis", Jahrbuch der Schiffbautechnischen Gesellschaft, Vol. 12, 1911, p. 283.

Frahm, H., "Results of trials of the anti-rolling tanks at sea", ", Transactions of the Institution of Naval Architects, Vol. 53, 1911, pp. 183-201.

Froude, W., "On the rolling of ships", Transactions of the Institution of Naval Architects, Vol. 2, 1861, pp. 180-227.

Gerrits, J., "Three-dimensional liquid sloshing in complex geometries", Master's Thesis, University of Groningen, Department of Mathematics, August 1996.

Gerrits, J., Loots, G.E., Fekken, G., and Veldman, A.E.P., "Liquid sloshing on earth and in space", In: Moving Boundaries V (B. Sarler, C.A. Brebbia and H. Power eds.) WIT Press, Southampton, 1999, pp. 111-120.

Gerrits, J. and Veldman, A.E.P., "Numerical simulation of coupled liquid-solid dynamics", European Congress on Computational Methods in Applied Sciences and Engineering (ECCOMAS), Barcelona (Spain), 2000.

Hirt, C.W. and Nichols, B.D., "Volume of Fluid (VOF) method for the dynamics of free boundaries", Journal of Computational Physics, Vol. 39, 1981, pp. 201-225.

Kleefsman, K.M.T., "Numerical simulation of ship motion stabilization by an activated U-tube anti-roll tank", Master's Thesis, University of Groningen, Department of Mathematics, August 2000.

Lee, B.S. and Vassalos, D., "An investigation into the stabilisation effects of anti-roll tanks with flow obstructions", International Shipbuilding Progress, Vol. 43, No. 433, 1996, pp. 70-88.

Loots, G.E., "Free surface flow in three-dimensional complex geometries", Master's Thesis, University of Groningen, Department of Mathematics, August 1997.

Loots, G.E., "Free surface flow in three-dimensional complex geometries using enhanced boundary treatment", Master's Thesis, University of Groningen, Department of Mathematics, June 1998.

Luth, H.R., "Design verification study for Dutch government patrol vessel", MARIN Report No. 67, 1999, p. 11.

Sabeur, Z., Cohen, J.E., Stephens, J.R. and Veldman, A.E.P., "Investigation on free surface flow oscillatory impact pressures with the Volume Of Fluid method", In: Numerical Methods in Fluid Dynamics VI (M.J. Baines ed.), Will Print, Oxford, 1998, pp. 493-498.

SHIPMO User's Guide, Maritime Research Institute Netherlands, 1998.

Stigter, C., "The performance of U-tanks as a passive anti-rolling device", TNO Report No. 81 S, February 1966.

Vasta, J., Giddings, A.J., Taplin, A. and Stilwell, J.J., "Roll stabilization by means of passive tanks", Transactions of the Society of Naval Architects and Marine Engineers, Vol. 69, 1961, pp. 411-460.

Verhagen, J.H.G. and Wijngaarden, L. van, "Non-linear oscillations of fluid in a container", Journal of Fluid Mechanics, Vol.22, Part 4, 1965, pp. 737-751.

Watts, P., "On a method of reducing the rolling of ships at sea", Transactions of the Institution of Naval Architects, Vol. 24, 1883, pp. 165-191.

Watts, P., "The use of water chambers for reducing the rolling of ships at sea", Transactions of the Institution of Naval Architects, 1885, p. 30.

Webster, W.C., "Analysis of the control of activated antiroll tanks", Transactions of the Society of Naval Architects and Marine Engineers (SNAME), Vol. 75, 1967, pp. 296-331.

Yamaguchi, S. and Shinkai, A., "An advanced adaptive control system for activated anti-roll tank", International Journal of Offshore and Polar Engineering, Vol. 5, No. 1, 1995, pp. 17-22.

Zhong, Z., Falzarano, J.M., and Fithen, R.M., "A numerical study of U-tube passive anti-roll tanks", Proceedings of the International Symposium of Offshore and Polar Engineering (ISOPE), Vol. 3, 1998, pp. 504-512.

DISCUSSION

A. Cariou
Institut de Recherche de la Construction Navale, France

Here the tank fluid motion simulation is fully non-linear. But the equations used for the coupling of the ship with the tank (equations (9) through (12)) are the equations of pure linear dynamics. Could you please comment on that point?

AUTHOR'S REPLY

The statement that the equations used for the coupling of the ship with the anti-roll tank are purely linear is not correct. The coupled equations of motion may seem to be linear with respect to the ship motions, but they are not! The forces exerted by the tank on the ship depend on the ship motions in a nonlinear way, which (I admit) has not been made explicit in equations 9-12. Yet, this is exactly the point where the nonlinearity comes into the time domain equations of motion.

DISCUSSION

A. Clement
Laboratoire Mècanique des Fluides, Ecole Centrale de Lyon, France

If I understand well, the principle of your control consists in changing the natural frequency of the tank to make it fit the frequency of the ship motion. This principle cannot be easily extended to irregular motions, except if you consider that you know the near future of the excitation by a suitable prediction of sophisticated control process as we do with active wave absorbers for wave basics. Did you include such a prediction algorithm in your active control?

AUTHOR'S REPLY

This is a very important observation which has our attention. We have not accounted for the effects of irregular waves (and motions) in our control algorithm. Undoubtedly, we will be forced to include a prediction algorithm once we start testing our method in irregular wave conditions.

DISCUSSION

M. Hirano
Mitsui Akishima Laboratory, Japan

Anti-rolling tanks are usually installed on a ship as a part of ship structure. In this sense, such small structural members as stiffeners may be fitted inside the tank wall. Question is whether the effects of stiffeners on both roll moment amplitude and phase angle can be computed or not in the computation?

AUTHOR'S REPLY

In principle this is possible, although it would require a very detailed grid and, consequently, a very powerful computer. Up to now, we have not investigated the effects of local three-dimensional geometry variations.